Discrete-time Modeling and Numerical Evaluation of BER Performance for A BPSK-based DCSK-Walsh Coding Communication System over Multipath Rayleigh Fading Channels

Doan Thi Que[1,2], Nguyen Xuan Quyen[1], Thang Manh Hoang[1*]

[1] *Hanoi University of Science and Technology – No. 1, Dai Co Viet Str., Hai Ba Trung, Ha Noi, Viet Nam*

[2]*Faculty of Information Technology, Hanoi National University of Education - 136 Xuan Thuy Street, Hanoi, VN*

Received: September 08, 2016; accepted: June 9, 2017

Abstract

This paper investigates the use of binary phase shift keying (BPSK) modulation for multiple-access communication systems based on differential chaos shift keying-Walsh Coding (DCSK-WC). This aims at converting the chaotic-modulated signal from low-frequency baseband into high frequency band before being transmitted on the channel. In the transmitter, a chaotic sequence is transformed into the non-return-to-zero (NRZ) form which is then fed into the BPSK modulation. The output of modulation, i.e., NRZ-Chaos/BPSK signal, is used as a spreading code in the DCSK-WC modulation. The process of data recovery in the receiver is performed by means of the correlation calculation and energy detection as in the conventional DCSK method. The mathematical model in discrete-time domain describes the operation of the transmitter and receiver over multipath Rayleigh fading channels. The Bit-error-rate performance of the system is evaluated by numerical simulation. The results show that the proposed BPSK/DCSK-WC system allows adjusting the operating frequency band with the use of BPSK, while still keeping the performance equivalent to that of the conventional one.

Keywords: BPSK, DCSK, Multiple access, Walsh code, Multipath channel.

1. Introduction

Among chaos-based digital communication systems, differential chaos-shift keying (DCSK) has been the most widely studied [1]-[6]. Owing to the simple structure, the DCSK system is promising for hardware implementation [7]. Furthermore, the synchronization of chaotic sequences is not required at the receiving side; hence the DCSK offers a good performance in multipath propagation environments [8]. The binary data is spread in the frequency domain with the use of a wideband chaotic signal which plays the role as a carrier. The principal purpose of the spread-spectrum is to overcome the multipath propagation problem and reduce the transmitted power spectral density. This reduction helps to minimize the interference to other radio channels in the same operating frequency band. For the spread-spectrum systems, multiple-access ability is a critical requirement to have efficient bandwidth of communication channel [9]. Several multiple-access techniques have been proposed for the DCSK system [10]-[14], where the technique based on Walsh-coding (DCSK-WC) has been received the most attention. In the DCSK-WC, each chaotic carrier is combined with two Walsh functions to create two orthogonal basis functions corresponding to bit "1" and "0".

In most of the chaos-based modulation schemes proposed previously, the chaotically-modulated signal at the output is directly transmitted on the channel [15]. The frequency range occupied on the channel depends on the bandwidth of the used chaotic carrier [16]. However, for a defined transmission channel, the communication systems have to convert the spectrum of the transmitted signal to the allowed or allocated frequency range. This spectrum conversion can be carried out by directly changing the parameters of the chaotic-carrier generator. However, owing to the dynamical behavior of chaotic generators, the change by this way is not easy. Addressing this problem is also the motivation for our study, where the idea of using a conventional narrow band-pass modulation method aiming at shifting the spectrum of the DCSK/WC-modulated signals is proposed. We present and investigate a BPSK/DCSK-WC communication system which is based on the combination of BPSK and DCSK-WC techniques. In the transmitter, the chaotic signal at the baseband is converted into the pass-band signal by means of BPSK before being processed with the DCSK-WC modulator. By this way, the spectrum of the transmitted signal is easily adjusted by changing the BPSK carrier frequency. In the receiver, the original data is recovered with the same steps as in

[*] Corresponding author: Tel.: (+84) 988802694
Email: thang.hoangmanh@hust.edu.vn

the conventional DCSK/WC demodulator, which employs the correlation calculation and energy detection. For the clarified description of our idea, discrete-time domain models of the transmitter, multipath Rayleigh fading channel, and receiver of the BPSK-DCSK/WC system are given and analyzed in detail. We evaluate the BER performance by numerical simulations to verify the feasibility of the proposed system.

2. Discrete-time Modeling of BPSK-DCSK/WC System

In this section, discrete model of the proposed BPSK/DCSK-WC system is presented and analyzed. Fig. 1 shows the block diagram of the system which consists of the transmitter, generalized multipath Rayleigh fading channel, and receiver.

2.1. Transmitter

Let us consider the u^t transmitter. The chaotic sequences at the output of the chaotic generators are produced by a chaotic map with different initial values. The output signal of chaotic generator, denoted by $c_u(t)$, is converted into the non return-to-zero data format given by

$$d_u(t) = \begin{cases} 1 & \text{if } c_u(t) \geq 0, \\ -1 & \text{if } c_u(t) < 0. \end{cases} \quad (1)$$

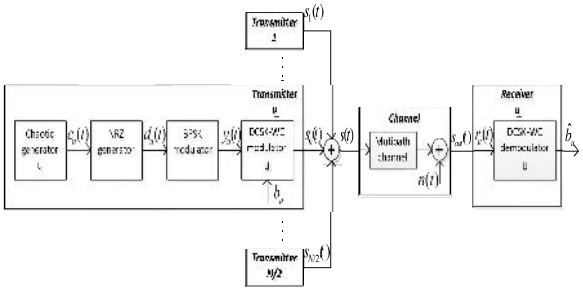

Fig. 1. The block diagram of the proposed BPSK/DCSK-WC system.

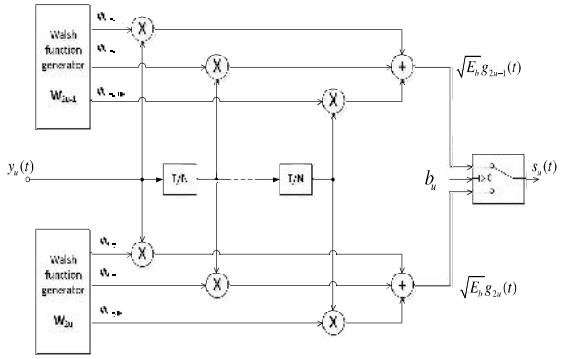

Fig. 2. The structure of the DCSK-WC modulator.

In the BPSK modulator, the input signal $d_u(t)$ is multiplied by a sinusoidal carrier, i.e., $s_u(t) = s_u \cos(2\pi f_u t)$ to generate a pass-band signal as follows:

$$y_u(t) = \begin{cases} s_u \cos(2\pi f_u t) & \text{if } d_u(t) = 1, \\ -s_u \cos(2\pi f_u t) & \text{if } d_u(t) = -1, \end{cases} \quad (2)$$

where s_u and f_u are the amplitude and frequency of the carrier, respectively. This signal is then fed into the conventional DCSK-WC modulator. The structure of the DCSK-WC modulator is shown in Fig. 2, in which two Walsh functions w_{2u-1} and w_{2u} generated from a Walsh matrix of the orthogonal functions are used to generate two orthogonal basis functions $g_{2u-1}(t)$ and $g_{2u}(t)$ corresponding to bit "1" and "0" of the u^t user, respectively. In this system, the number of users is denoted by $N/2$, thus it needs using N Walsh functions w_j with $(j = 1,2,\dots,N)$. Let $w_{j,k}$ with $k = 1,2,\dots,N$ denotes the segments of j^t Walsh function, then we have

$$\frac{1}{N}\sum_{k=1}^{N} w_{j,k} w_{l,k} = \begin{cases} 1 & j = l, \\ 0 & j \neq l. \end{cases} \quad (3)$$

The output signal of the DCSK-WC modulator at u^t user is expressed by

$$s_u(t) = \begin{cases} \sqrt{E_b} g_{2u-1}(t) & \text{if } b_u = 1, \\ \sqrt{E_b} g_{2u}(t) & \text{if } b_u = 0, \end{cases}$$
$$= \begin{cases} \sqrt{E_b}\sum_{k=1}^{N} w_{2u-1,k} y_{u,k}(t-(k-1)\frac{T}{N}) & \text{if } b_u = 1, \\ \sqrt{E_b}\sum_{k=1}^{N} w_{2u,k} y_{u,k}(t-(k-1)\frac{T}{N}) & \text{if } b_u = 0, \end{cases} \quad (4)$$

where b_u is the transmitted data of u^t transmitter.

Based on the result in Equation (4), the output signal at the DCSK-WC modulators is calculated by sum

$$s(t) = \sum_{u=1}^{\frac{N}{2}} s_u(t)$$
$$= \begin{cases} \sqrt{E_b}\sum_{u=1}^{N/2}\sum_{k=1}^{N} w_{2u-1,k} y_{u,k}(t-(k-1)\frac{T}{N}) & \text{if } b_u = 1, \\ \sqrt{E_b}\sum_{u=1}^{N/2}\sum_{k=1}^{N} w_{2u,k} y_{u,k}(t-(k-1)\frac{T}{N}) & \text{if } b_u = 0. \end{cases} \quad (5)$$

2.2. Channel

The most popular model of a multipath fading channel is a tapped delay line model [17], which is shown in Fig. 3, where L is the number of the paths, α_i and τ_i with $i = 1,2,\dots,L$ are gain and delay of the i^t path, respectively. Here, the gain coefficients α_i are independent and Rayleigh distributed random variables expressed by

$$f(\alpha_i) = \frac{\alpha_i}{\sigma_i^2} e^{-\alpha_i^2/(2\sigma_i^2)}, \qquad \alpha_i \geq 0, \quad (6)$$

where σ_i is the scale parameter of the distribution. Here, we consider time-flat fading channels, which mean the gain keeps constant at least in one bit

duration. Hence, the output signal of the channel is given by sum

$$S_o\ (t) = \sum_{i=1}^{L} \alpha_i\, s(t-\tau_i) + n(t), \tag{7}$$

where $n(t)$ is additive white Gaussian noise (AWGN).

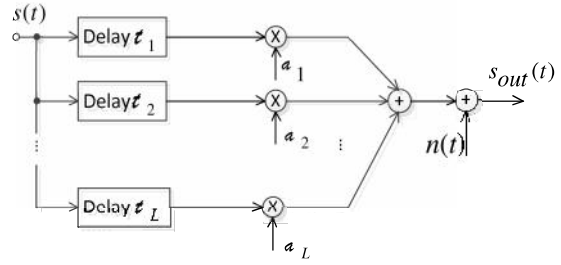

Fig. 3. Tapped delay line model of multipath fading channel.

2.3. Receiver

The input signal of the u^t receiver, denoted by $r_u(t)$, is the output signal of the channel. Based on Equations (5) and (7), we can derive as follows:

$$r_u(t) = s_o\ (t)$$
$$= \begin{cases} \sqrt{E_b}\sum_{i=1}^{L}\alpha_i \sum_{u=1}^{N/2}\sum_{k=1}^{N} w_{2\ -1,k}\, y_{u,k}\left(t-(k-1)\frac{T}{N}-\tau_i\right)+\cdots \\ \qquad n(t) \qquad \text{if } b_u = 1, \\ \sqrt{E_b}\sum_{i=1}^{L}\alpha_i \sum_{u=1}^{N/2}\sum_{k=1}^{N} w_{2\ ,k}\, y_{u,k}\left(t-(k-1)\frac{T}{N}-\tau_i\right)+\cdots \\ \qquad n(t) \qquad \text{if } b_u = 0. \end{cases} \tag{8}$$

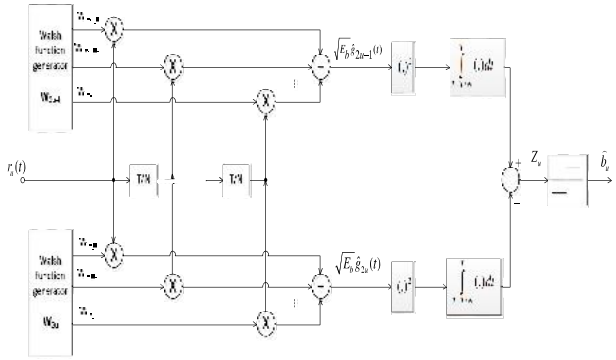

Fig. 4. The block diagram of the energy detector.

The received signal is put into the u^t DCSK-WC demodulator. There are two different detectors for the demodulation proposed in [18], which are the coherent correlation detector and the energy detector. In the first approach, the carrier is reproduced at the receiver and required to synchronize with the incoming signal. However, the synchronization of chaotic sequences over multipath propagation environments is a big challenge in chaos-based communications. Therefore, the second approach is used in our proposal. The block diagram of the energy detector is shown in Fig. 4.

Two restored orthogonal basis functions of the u^t user $\hat{g}_{2\ -1}(t)$ and $\hat{g}_2\ (t)$ are written as

$$\sqrt{E_b}\hat{g}_{2\ -1}(t) = \sum_{k=1}^{N} w_{2\ -1,N+1-k}\, r_{u,k}\left((k-1)\frac{T}{N}\right)$$
$$= \begin{cases} \sum_{k=1}^{N} W_{2\ -1,N+1-k}\left(\sqrt{E_b}\sum_{l=1}^{L}\alpha_l \sum_{v=1}^{\frac{N}{2}}\sum_{k=1}^{N} w_{2\ -1,k}\cdots \right. \\ \qquad \left. y_{v,k}\left(t-(k-1)\frac{T}{N}-\tau_l\right)+n_{u,k}(t-(k-1)\frac{T}{N})\right) \quad \text{if } b_u = 1, \\ \sum_{k=1}^{N} W_{2\ -1,N+1-k}\left(\sqrt{E_b}\sum_{l=1}^{L}\alpha_l \sum_{v=1}^{\frac{N}{2}}\sum_{k=1}^{N} w_{2\ ,k}\cdots \right. \\ \qquad \left. y_{v,k}\left(t-(k-1)\frac{T}{N}-\tau_l\right)+n_{u,k}(t-(k-1)\frac{T}{N})\right) \text{ if } b_u = 0, \end{cases} \tag{9}$$

and

$$\sqrt{E_b}\hat{g}_2\ (t) = \sum_{k=1}^{N} w_{2\ ,N+1-k}\, r_{u,k}\left((k-1)\frac{1}{N}\right)$$
$$= \begin{cases} \sum_{k=1}^{N} W_{2\ ,N+1-k}\left(\sqrt{E_b}\sum_{l=1}^{L}\alpha_l \sum_{v=1}^{\frac{N}{2}}\sum_{k=1}^{N} w_{2\ -1,k}\cdots \right. \\ \qquad \left. y_{v,k}\left(t-(k-1)\frac{1}{N}-\tau_l\right)+n_{u,k}(t-(k-1)\frac{1}{N})\right) \text{ if } b_u = 1, \\ \sum_{k=1}^{N} W_{2\ ,N+1-k}\left(\sqrt{E_b}\sum_{l=1}^{L}\alpha_l \sum_{v=1}^{\frac{N}{2}}\sum_{k=1}^{N} w_{2\ ,k}\cdots \right. \\ \qquad \left. y_{v,k}\left(t-(k-1)\frac{1}{N}-\tau_l\right)+n_{u,k}(t-(k-1)\frac{1}{N})\right) \quad \text{if } b_u = 0. \end{cases} \tag{10}$$

According to Eq. (3), we have

$$\frac{1}{N}\sum_{k=1}^{N} w_{2\ -1,N+1-k} w_{2\ -1,k} = \begin{cases} 1 & \text{if } u = v \text{ and } b_u = b_v, \\ 0 & \text{if } u \neq v, \end{cases} \tag{11}$$

and

$$\frac{1}{N}\sum_{k=1}^{N} w_{2\ -1,N+1-k} w_{2\ ,k} = 0, \quad \forall\, u, v. \tag{12}$$

On the basis of equations (9), (11) and (12), we obtain the following result:

$$\sqrt{E_b}\hat{g}_{2\ -1}(t) =$$
$$\begin{cases} N\sqrt{E_b}\sum_{i=1}^{L}\alpha_i\, y_u\left(t-\frac{T}{N}-\tau_i\right)+\cdots \\ \quad \sum_{k=1}^{N} w_{2\ -1,N+1-k}\, n_{u,k}\left(t-(k-1)\frac{T}{N}\right) \quad \text{if } b_u = 1, \\ \sum_{k=1}^{N} w_{2\ -1,N+1-k}\, n_{u,k}\left(t-(k-1)\frac{T}{N}\right) \quad \text{if } b_u = 0. \end{cases} \tag{13}$$

Similarly, computation of $\hat{g}_2\ (t)$ is same as that of $\hat{g}_{2\ -1}(t)$, we get

$$\sqrt{E_b}\hat{g}_2\ (t) =$$
$$\begin{cases} \sum_{k=1}^{N} w_{2\ ,N+1-k}\, n_{u,k}(t-(k-1)\frac{T}{N}) \quad \text{if } b_u = 1, \\ -N\sqrt{E_b}\sum_{i=1}^{L}\alpha_i\, y_u\left(t-\frac{T}{N}-\tau_i\right)+\cdots \\ \quad \sum_{k=1}^{N} w_{2\ ,N+1-k}\, n_{u,k}\left(t-(k-1)\frac{T}{N}\right) \quad \text{if } b_u = 0. \end{cases} \tag{14}$$

The observation signal $Z_u(t)$ in the diagram in Fig. 4 is written as

$$Z_u(t) = \int_{T-T/N}^{T}\left(\sqrt{E_b}\hat{g}_{2\ -1}(t)\right)^2 dt - \int_{T-T/N}^{T}\left(\sqrt{E_b}\hat{g}_{2\ }(t)\right)^2 dt, \quad (15)$$

where

$$\int_{1-\frac{1}{N}}^{1}\left(\sqrt{E_b}\hat{g}_{2\ -1}(t)\right)^2 dt = \begin{cases} \int_{1-1/N}^{1}\left(\begin{matrix} N\sqrt{E_b}\sum_{l=1}^{L}\alpha_l y_u\left(t-\frac{1}{N}-\tau_l\right) \\ +\sum_{k=1}^{N} w_{2\ -1,N+1-k} n_{u,k}(t-(k-1)\frac{1}{N}) \end{matrix}\right)^2 dt & \text{if } b_u = 1, \\ \int_{1-1/N}^{1}\left(\sum_{k=1}^{N} w_{2\ -1,N+1-k} n_{u,k}(t-(k-1)\frac{1}{N})\right)^2 dt & \text{if } b_u = 0, \end{cases} \quad (16)$$

and

$$\int_{1-1/N}^{1}\left(\sqrt{E_b}\hat{g}_{2\ }(t)\right)^2 dt = \begin{cases} \int_{1-1/N}^{1}\left(\sum_{k=1}^{N} w_{2\ ,N+1-k} n_{u,k}(t-(k-1)\frac{1}{N})\right)^2 dt & \text{if } b_u = 1, \\ \int_{1-1/N}^{1}\left(\begin{matrix} -N\sqrt{E_b}\sum_{l=1}^{L}\alpha_l y_u\left(t-\frac{1}{N}-\tau_l\right) \\ +\sum_{k=1}^{N} w_{2\ ,N+1-k} n_{u,k}\left(t-(k-1)\frac{1}{N}\right) \end{matrix}\right)^2 dt & \text{if } b_u = 0. \end{cases} \quad (17)$$

In noise-free case, the observation signal is calculated as follows:

$$Z_u(t) = \begin{cases} \int_{T-T/N}^{T}\left(N\sqrt{E_b}\sum_{l=1}^{L}\alpha_l y_u(t-\frac{T}{N}-\tau_l)\right)^2 dt & \text{if } b_u = 1, \\ -\int_{T-\frac{T}{N}}^{T}\left(-N\sqrt{E_b}\sum_{l=1}^{L}\alpha_l y_u\left(t-\frac{T}{N}-\tau_l\right)\right)^2 dt & \text{if } b_u = 0. \end{cases} \quad (18)$$

Equation (18) points out that, $z_u(t) > 0$ when bit "1" is transmitted and vice versa. Hence, the binary data at the output of the u^t demodulator is recovered by the following rule:

$$\tilde{b}_u = \begin{cases} 1 & \text{if } Z_u(t) > 0, \\ 0 & \text{if } Z_u(t) < 0. \end{cases} \quad (19)$$

3. Simulation Results and Discussion

In this section, BER performance of the proposed system is evaluated by simulation in Simulink over multipath Rayleigh Fading channels with AWGN. We study the dependence of BER performance upon the system parameters such as number of users and different chaotic maps. Here, the simulated BERs are calculated as the number of error bits divided by total number 10^6 bits transmitted. In all simulations, we assume that two-path Rayleigh fading channel model is used with $\tau_1 = 0$ ns, $\tau_2 = 75$ ns, $E\{(\alpha_1)^2\} = E\{(\alpha_2)^2\} = \frac{1}{2}$, bit duaration $T = 2$ µs. These parameters have been selected for office building in WLAN applications (detailed reasons for choosing these parameters can be found in [8].

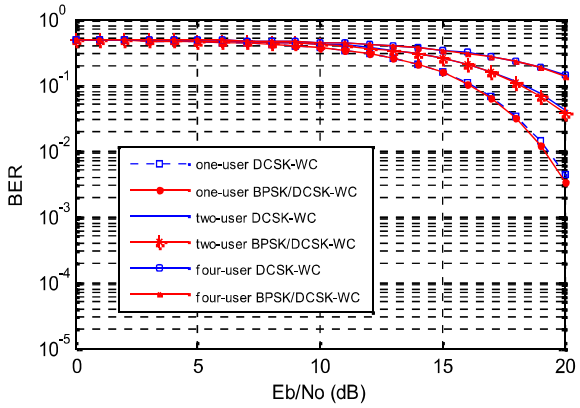

Fig. 5. BER performance of the BPSK/DCSK-WC and DCSK-WC system over two-path Rayleigh Fading channels with $2M = 200$, $\tau_1 = 0$ ns, $\tau_2 = 75$ ns, $E\{(\alpha_1)^2\} = E\{(\alpha_2)^2\} = \frac{1}{2}$.

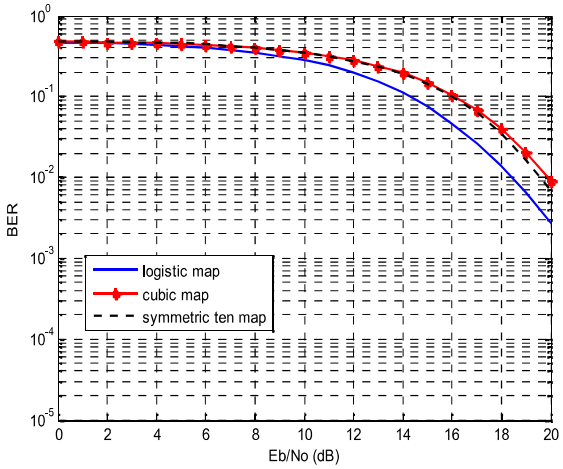

Fig. 6. BER performance in a two-user BPSK/DCSK-WC system. Symmetric Tent map, Cubic map and ogistic map are used, respectively. $2M = 80$.

Firstly, the BER performance of the DCSK-WC and BPSK/DCSK-WC systems are displayed. All chaotic signals are generated by the same symmetric ten map [19] but with different initial conditions. Fig. 5 shows BERs against E_b/N_0 for one-user, two-user and four-user systems with spreading factor $2M = 200$, respectively. These results point out that, the BER performance of the proposed BPSK/DCSK-WC system is equivalent to that of the DCSK-WC system. For instance, in the two-user system, at the same $\frac{E_b}{N_0} = 18$ dB, the BERs for BPSK/DCSK-WC and DCSK-WC are about 0.109 and 0.113, respectively.

Secondly, the BER performance of BPSK/DCSK-WC system is investigated with the symmetric ten map, cubic map and logistic map, which are used regularly to evaluate the performance of DCSK system [19], [20]. Fig. 6 shows the results

for the two-user system with the spreading factor $2M = 80$ when symmetric ten map, cubic map and logistic map are used, respectively. It can be observed that using logistic map produces a lower BER, while the BERs of the users using cubic map and symmetric ten map are the same.

4. Conclusion

In this paper, we have presented and investigated the combination scheme of BPSK and DCSK-WC for digital communication. The proposed scheme in the form of the bock diagrams for the transmitter, channel and receiver is described in detail by means of their discrete-time mathematical models. The performance of the proposed system is determined by simulation results in terms of the BER values against the typical parameters of system. It can be seen from the obtained results that the combination scheme not only adjust the operating frequency band with the use of BPSK but also maintains an approximately BER performance in comparison to that of the conventional one. The determination of theoretical performance to validate the obtained simulation results are our future work.

Acknowledgements

This research is funded by Vietnam National Foundation for Science and Technology Development (NAFOSTED) under grant number 102.02-2012.27.

References

[1] G. Kolumban, B. Vizvári, W. Schwarz, A. Abel, Differential chaos shift keying: A robust coding for chaos communications, Proc. NDES'96, pp. 87–92, 1996.

[2] G. Kolumbán, G. Kis, Z. Jákó, M.P. Kennedy, FM-DCSK: A robust modulation scheme for chaotic communications, IEICE Trans. Fund., vol. E81-A, pp. 1798–1802, 1998.

[3] Y.Xia, C.K. Tse, F.C.M. Lau, Performance of differential chaos-shift-keying digital communication systems over a multipath fading channel with delay spread, IEEE Trans. Circuits Syst. II: Exp. Briefs, vol. 51, no. 12, pp. 680–684, 2004.

[4] G. Cai, L. Wang, T. Huang, Channel capacity of M-ary Differ-ential Chaos Shift Keying modulation over AWGN channel, Proc.Int. Symp. Commun. Inf. Technol. (ISCIT), pp. 91–95, 2013.

[5] W. Xu, L. Wang, G. Chen, Performance analysis of the CS-DCSK/BPSK communication system, IEEE Transactions on Circuits and Systems I: Regular Papers, vol. 61(9), pp. 2624-2633, 2014.

[6] N. Quyen, T.Q. Duong, A. Nallanathan, Modeling, Analysis and Performance Comparison of Two Direct Sampling DCSK Receivers under Frequency Nonselective Fading Channels, IET Communications, vol. 10 (11), pp. 1263 – 1272, 2016.

[7] M. Delgado-Restituto, A. J. Acosta, A. Rodriguez-Vazquez, A mixed-signal integrated circuit for FM-DCSK modulation, IEEE Journal of Solid-State Circuits, vol. 40, pp. 1460-1471, 2005.

[8] M.P. Kennedy, G. Kolumbán, G. Kis, Z. Jákó, Performance evaluation of FM-DCSK modulation in multipath environments, IEEE Trans. Circuits Syst. I, vol. 47, pp. 1702–1711, 2000.

[9] R.L. Peterson, R.E. Ziemer, D.E. Borth, Introduction to Spread Spectrum Communications, vol. 995, New Jersey: Prentice Hall, 1995.

[10] G. Kolumban, M.P. Kennedy, G. Kis, Multilevel differential chaos shift keying, Proc. NDES'97, pp. 191-196, 1997.

[11] F.C.M. Lau, M.M. Yip, C.K. Tse, S.F. Hau, A multiple access technique for differential chaos shift keying, IEEE Trans. Circuits Syst. I, vol. 49, pp. 96–104, 2002.

[12] F.C.M. Lau, K.Y. Cheong, C.K. Tse, Permutation-Based DCSK and Multiple-Access DCSK Systems, IEEE Trans. Circuits Syst. I, vol. 50, pp. 733-742, 2003.

[13] P. Chen, L. Wang, G. Chen, DDCSK-Walsh Coding: A Reliable Chaotic Modulation-Based Transmission Technique, IEEE Trans. Circuits Syst. II, vol. 59, pp. 128–132, 2012.

[14] G. Kolumbán, M.P. Kennedy, Z. Jákó, G. Kis, Chaotic communications with correlator receiver: Theory and performance limit, Proceedings of the IEEE, vol 90, pp. 711–732, 2002.

[15] P. Stavroulakis, Chaos Applications in Telecommunications, CRC Press, 2005.

[16] F.C.M. Lau, C.K. Tse, Chaos-Based Digital Communication Systems: Operating Principles, Analysis Methods, and Performance Evaluation, Springer, New York, 2003.

[17] A.F. Molisch, Wireless Communications, 2nd ed. Wiley, 2011.

[18] G. Kis, Performance analysis of chaotic communications systems, PhD thesis, 2003.

[19] M. Sushchik, L.S. Tsimring, A.R. Volkovskii, Performance analysis of correlation-based communication schemes utilizing chaos, IEEE Trans. Circuits Syst. I, vol. 47, pp. 1684-1691, 2000.

[20] W.M. Tam, F.C.M. Lau, C.K. Tse, Analysis of bit error rates for multiple access CSK and DCSK communication systems, IEEE Trans. Circuits Syst. I, vol. 50, pp. 702-707, 2003.